Assessment of Temporal Variations in Crop Growth Dynamics Using UAV Imagery

Ayyappa Reddy Allu[1,*] and Shashi Mesapam[2]

[1]Department of Civil Engineering, National Institute of Technology, Warangal, Telangana, India – aa721015@student.nitw.ac.in
[2]Department of Civil Engineering, National Institute of Technology, Warangal, Telangana, India – mshashi@nitw.ac.in

Keywords: Unmanned Aerial Vehicle, Crop Monitoring, Vegetation Indices, Canopy Height.

Abstract

Effective crop monitoring is essential for optimizing agricultural practices and promoting sustainable production. This study explores the use of temporal Unmanned Aerial Vehicle (UAV) imagery to assess variations in crop growth dynamics across different developmental stages. UAV images were captured at five-day intervals, enabling the analysis of temporal changes in phenological parameters and plant health. Key vegetation indices and canopy height were derived at multiple time points and statistically evaluated to determine their effectiveness in monitoring crop development. The multi-temporal analysis identified the most informative vegetation indices and image processing techniques for assessing crop conditions. Results demonstrate that UAV-based temporal imaging offers valuable insights into crop growth patterns that are difficult to obtain through conventional monitoring approaches. The findings highlight the potential of UAV imagery as a practical tool for improving crop management by enabling timely and informed decision-making, ultimately contributing to enhanced yield and resource use efficiency.

1. Introduction

Crop monitoring is essential for ensuring food security, optimizing agricultural productivity, and managing resources effectively. Regular monitoring of crop health, growth, and yield allows farmers and agronomists to identify potential issues early, enabling timely interventions to minimize crop losses and enhance yields. Remote sensing data serves as a valuable tool for capturing detailed information about crops over large areas, often with high frequency (Allu & Mesapam, 2024). While satellite images are highly useful for monitoring crop health on a large scale, they may not provide sufficient detail at the individual plant level. In contrast, UAVs (Unmanned Aerial Vehicles) offer high-resolution images capable of capturing detailed crop information at the plant level (Yeom et al., 2019).

UAV based monitoring offers a valuable means to assess crop health, monitor irrigation efficiency, and differentiate between tillage practices, all of which contribute to improving agricultural productivity and sustainability. In this context, vegetation indices (VIs) derived from UAV data have proven to be a powerful tool for assessing crop performance and environmental conditions. Several studies have demonstrated the utility of different UAV-based sensors, including RGB (Red-Green-Blue), NIR (Near-Infrared), and thermal imaging, in capturing detailed crop characteristics that cannot be observed through traditional ground-based methods. NIR-based vegetation indices were more effective in capturing the differences between conventional tillage and no-tillage fields, particularly in sorghum fields, where RGB-based indices failed to distinguish tillage treatments (Yeom et al., 2019). UAV based thermal imaging sensors are capable to provide real-time estimates of evapotranspiration, particularly when canopy cover was variable. The UAV-derived data were compared with traditional on-farm irrigation efficiency measurements, showing that UAV-based thermal imaging was an effective and reliable method for assessing irrigation performance and water usage in orchards (Garcia-Vasquez et al., 2022).

Several studies have demonstrated the utility of VIs derived from RGB imagery for monitoring various crops, including rice, sugarcane, and wheat, providing insights into crop health, biomass estimation, and growth patterns (Gerardo & De Lima, 2023). VIs could be effectively applied to rice crop monitoring, particularly in the late vegetative phase, even in the absence of multispectral imagery. Similarly, Ruwanpathirana et al., (2024) highlighted the success of machine learning models like Random Forest (RF) and Multiple Linear Regression (MLR) in predicting sugarcane growth parameters such as plant height, using RGB-based vegetation indices (VIs) like the Green Leaf Index (GLI) and VARI. These studies collectively underscore the potential of UAV based vegetation indices in enhancing crop monitoring accuracy and supporting sustainable agricultural practices.

The novelty of the study lies in evaluating the effectiveness of temporal UAV images for monitoring crop health parameters by exploring the relationships between various vegetation indices (NDVI, GNDVI, SAVI, EVI, and LAI) and canopy height. These relationships are analyzed metrics like RMSE, R^2, and Pearson's correlation coefficient (r) to evaluate the strength and accuracy of the models.

2. Study Area

The study area for cultivation is situated in Dharmasagar village, located in the Hanamkonda district of Telangana, India and the geographical location of the study area is illustrated in figure 1. In this region, farmers predominantly grow crops such as paddy, maize, cotton, and peanuts. The irrigation methods utilized in the area include both canal irrigation and groundwater irrigation, providing essential water resources to sustain agricultural practices throughout the year.

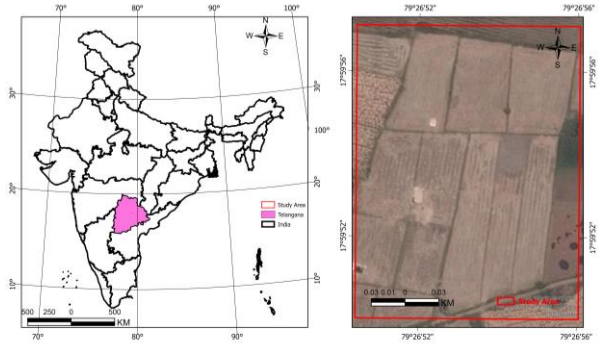

Figure 1. Study area

3. Methodology

The methodology of monitoring the crop using the temporal UAV images are presented in the figure 2.

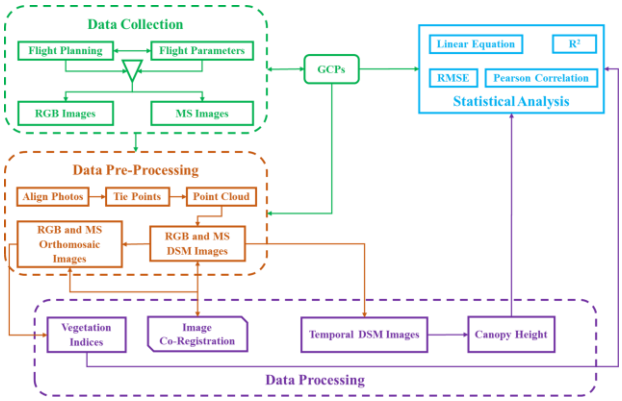

Figure 2. Methodology of monitoring the crop health

3.1 Data Collection

UAV (ideaForge Q4i) equipped with Parrot Sequoia multispectral sensor and sunshine sensor is used in this study to collect the multispectral images. UAV flown with a cruise speed of 7m/s and at an altitude of 70m above the ground reference and captured the images by maintaining an end lap and side lap of 80%. The flight planning of UAV was done in the BlueFire Touch software.

Table 1. UAV flight planning parameters and sensor characteristics

Altitude	70m	Band Name	Wavelength
End Lap	80%	Green	550nm ± 40nm
Side Lap	80%	Red	660nm ± 40nm
Cruise Speed	7m/s	Red-Edge	735nm ± 10nm
UAV size with propeller	< 80cm x 80cm	Near Infrared	790nm ± 40nm
UAV weight	< 3.5 Kgs	RGB	Red
Flight Planning Platform	BlueFire Touch		Green
Multispectral Sensor	Parrot Sequoia		Blue

Parrot Sequoia is a multispectral sensor and it captures the multispectral images (Green, Red, Red Edge and NIR) and RGB images. The multispectral sensor is installed under the UAV, facing the crops. It is powered directly by the UAV. The sunshine sensor is used to calibrate the images depending on the sunlight. This makes it possible to compare photos over time, despite variations in light during photo shoots. The sunshine sensor is attached on the upper part of the drone, facing the sky. During flights the sunshine sensor is powered by the multispectral sensor. Based on the flight planning parameters UAV images are collected at frequent interval of 5 days and it is stated from March 03, 2024 to April 27, 2024. The sensor characteristics of the multispectral sensor and UAV flight planning parameters are presented in Table 1.

In the location of the study area, paddy cultivation is started at the middle of January 2024. Canopy height information is collected from the field using the Differential Global Positioning System (DGPS) equipment and measuring scale. DGPS equipment used to collect the latitude, longitude and elevation of ground position and measuring scale is used to collect the actual canopy height in the field.

3.2 Data Pre-processing

The collected UAV images are acquired the camera position and altitude (latitude, longitude, elevation, omega, phi, and kappa) information from the inbuilt GPS and IMU sensor. The detailed steps of data collection and processing of temporal UAV images are presented in the figure 3. These camera positions were used to determine the coordinates of the imagery location including the quadcopter's roll, yaw, and pitch movements. The images were then aligned based on inertial measurements using the ground control points established using GPS. Once the images were aligned, tie points were generated from the common points between the images, which were used to orient the images. A dense point cloud was constructed by reconstructing the model using the tie points of the images and it was used to generate Digital Surface Model (DSM) which is helpful to generate orthomosaic images of RGB and MS images. Spatial resolution (in cm/pixel) of the generated temporal UAV images are presented in Table 2.

Table 2. Spatial resolution of temporal UAV images

Date of the Year	RGB	MS, DSM, and DTM
3/3/2024	2.24	7.74
8/3/2024	1.65	5.77
13/02/2024	1.86	6.41
18/03/2024	1.74	6.08
23/03/2024	1.76	6.1
28/03/2024	1.71	6
2/4/2024	1.75	6.12
7/4/2024	1.79	6.14
12/4/2024	1.75	6.22
27/04/2024	1.72	5.96

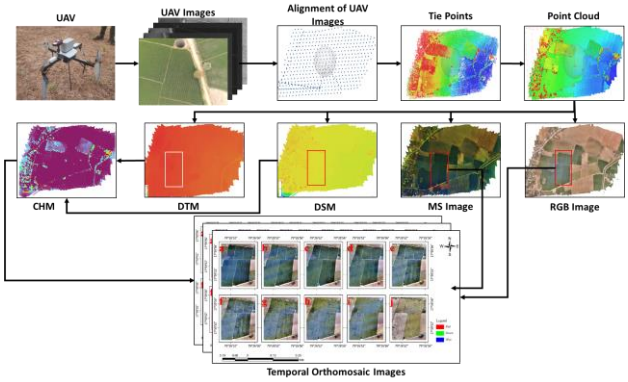

Figure 3. Data collection and processing of temporal UAV Images

These temporal UAV images are resampled to 6 cm/pixel and co-registered with other using the GCP's from the Differential Global Positioning System instrument for maintaining the consistency between the images.

3.3 Data Processing

Phenological parameters and vegetation indices (VIs) are very much helpful for monitoring the crop health. Canopy height is extracted from the canopy height model (CHM) which can be generated by subtracting the DTM of reference image from DSM of particular date. Canopy height is helpful for monitoring the phenological parameters. VIs are generated by performing the empirical analysis using bands of UAV orthomosaic images.

Indices	Equation	Application	Ref.
Normalized Difference Vegetation Index (NDVI)	$\frac{(NIR - Red)}{(NIR + Red)}$	Monitor the growth and health of vegetation and to identify areas of stress or damage	Jiang et al., 2021
Green Normalized Difference Vegetation Index (GNDVI)	$\frac{(NIR - Green)}{(NIR + Green)}$	Estimate chlorophyll content in leaves, making it useful for assessing nitrogen levels and photosynthetic activity in crops.	Mangewa et al., 2022
Soil Adjusted Vegetation Index (SAVI)	$\frac{(NIR - Red)}{(NIR + Red + L)} \times (1 + L)$	Evaluate vegetation health in areas with sparse vegetation, as it adjusts for soil brightness to provide a clearer indication of plant condition in soil-influenced environments	Huete, 1988
Enhanced Vegetation Index (EVI)	$\frac{2.5 \times (NIR - Red)}{(NIR + 6 \times Red - 7.5 \times Blue + 1)}$	Monitoring crop canopy structure and biomass	Sishodia et al., 2020
Leaf Area Index (LAI)	$3.618 \times EVI - 0.118$	Estimations of crop growth, canopy density, and potential photosynthetic activity	Boegh et al., 2002
CHM	$DSM - DTM$	Monitoring plant growth dynamics, detecting areas with stunted growth, and assessing crop parameters.	de Castro et al., 2021

3.4 Data Processing

Spatio-temporal statistical analysis between the canopy height and VIs is helps to establish the relationship between the structural and physiological characteristics of crops which is helpful for monitoring the agriculture at various stages. Analyzing the correlation and patterns between structural information (canopy height) with physiological metrics (VIs) enables more effective stress detection, yield prediction, remote sensing data validation, and optimization of agricultural management practices. For performing the statistical analysis, data was extracted from the 20 known location points from each dataset using R Studio software. Some common statistical metrics used in this context are Root Mean Square Error, Pearson correlation coefficient, linear equation and the coefficient of determination.

RMSE is a widely used metric that quantifies the differences between the indices (Ma et al., 2020). A lower RMSE value indicates a better fit between two variables, thus demonstrating the model's accuracy in estimating crop parameters such as chlorophyll content, moisture levels. The coefficient of determination (R^2) is another essential statistical measure that provides insight into how well the independent variable(s) explain the variability of the dependent variable (Mangewa et al., 2022). R^2 values range from 0 to 1, with values closer to 1 indicating that a significant proportion of the variability in the dependent variable is explained by the model. In the context of crop monitoring, a high R^2 value would imply that the UAV data effectively captures the variation in crop parameters, reinforcing the model's predictive power. Pearson correlation coefficient (r) measures the linear correlation between two variables, indicating how closely the relationship aligns with a straight line (Somvanshi & Kumari, 2020). The Pearson coefficient ranges from -1 to 1, where values closer to 1 indicate a strong positive correlation, values near -1 indicate a strong negative correlation, and values around 0 suggest no correlation. Empirical equations of the RMSE, R2, and Pearson correlation coefficient are expressed using the Eq. (1), (2) and (3) respectively.

$$RMSE = \sqrt{\frac{\sum_{i=1}^{n}(\text{Variable 1} - \text{Variable 2})^2}{n}} \quad (1)$$

$$R^2 = 1 - \frac{\text{sum of squares of residuals}}{\text{total sum of squares}} \quad (2)$$

$$r = \frac{\sum_{i=1}^{n}(x_i - \bar{x})(y_i - \bar{y})}{\sqrt{\sum_{i=1}^{n}(x_i - \bar{x})^2}\sqrt{\sum_{i=1}^{n}(y_i - \bar{y})^2}} \quad (3)$$

In this equation, x_i and y_i are the individual sample points, and $\bar{x}$ and $\bar{y}$ are the means of the respective datasets and n is the total number of observations.

4. Results and Discussions

The co-registered temporal UAV orthomosaic images of RGB and MS are presented in figure 4 and 5 respectively. The temporal analysis of UAV-derived vegetation indices revealed

dynamic changes across the observed dates, providing insights into crop growth and health. Temporal variations of the various VIs are represented in the violin plot (figure 6) and the mean values of the vegetation indices are presented in the figure 7. The NDVI values increased from a mean of 0.43 on March 3 to a peak of 0.69 on March 23, indicating vigorous growth during this period. The maximum NDVI value reached 0.91 on March 18, suggesting optimal photosynthetic activity. Similarly, GNDVI, SAVI, EVI, and LAI showed rising trends, with LAI peaking at 3.57 on March 18, reflecting dense canopy coverage. Standard deviations for all indices remained moderate, with LAI showing the highest variability, especially on March 18 (1.44), possibly due to heterogeneous crop growth conditions. The elevated mean values of SAVI and EVI between March 13 and March 28 highlight the period of enhanced vegetation cover and soil moisture retention, critical for crop productivity.

From April 2 onwards, a gradual decline in vegetation indices was observed, indicating the senescence phase as crop growth slowed. On April 27, NDVI, GNDVI, SAVI, EVI, and LAI reduced to mean values of 0.10, 0.12, 0.15, 0.09, and -0.10, respectively, with minimal variability. The maximum NDVI and GNDVI values dropped to 0.33 and 0.34, respectively, reflecting reduced photosynthetic activity. The negative mean LAI by April 27 implies a considerable decline in leaf area, corroborating the crop maturation and completion of the growing cycle. The statistical analysis highlights critical growth phases and suggests that UAV-based indices can effectively monitor crop health, informing timely agricultural management practices.

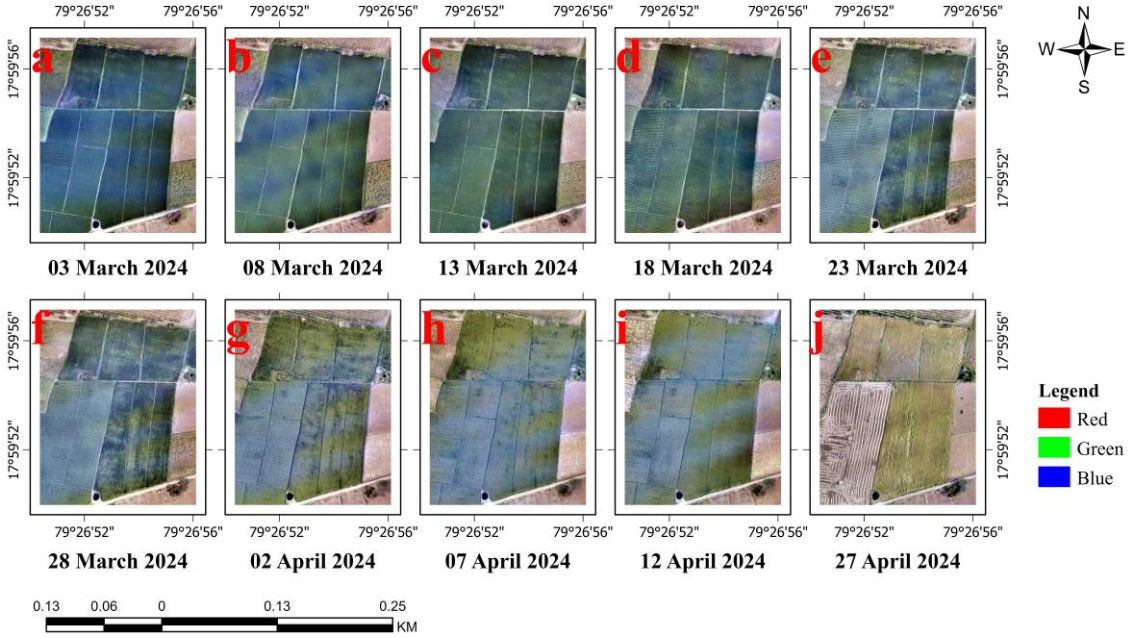

Figure 4. Temporal images of UAV RGB orthomosaic

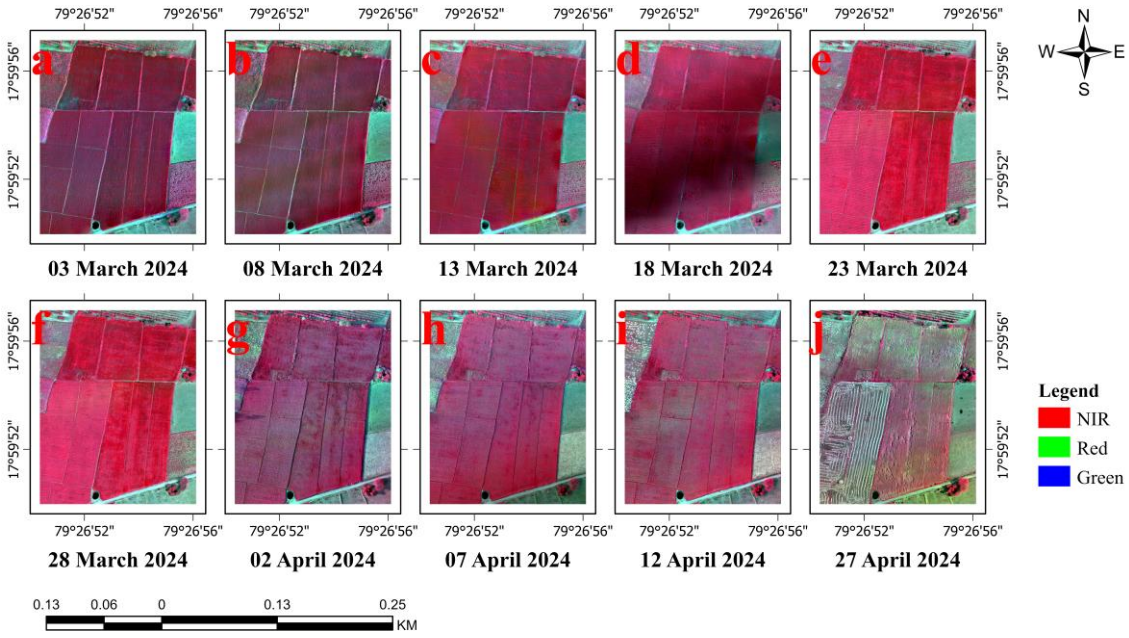

Figure 5. Temporal images of UAV Multispectral orthomosaic

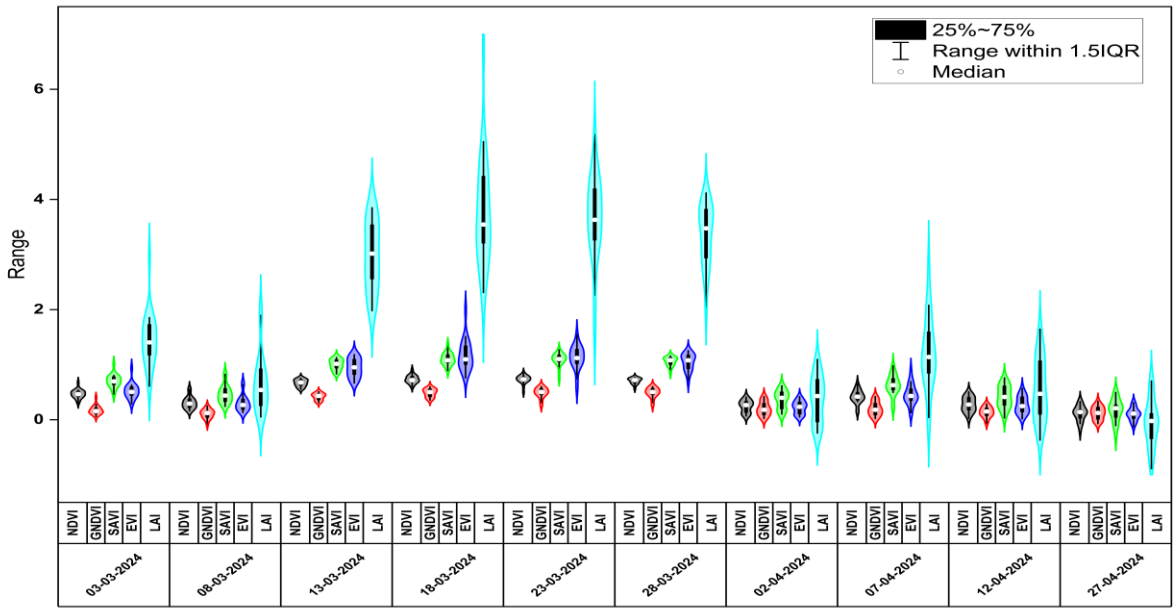

Figure 6. Indices value range

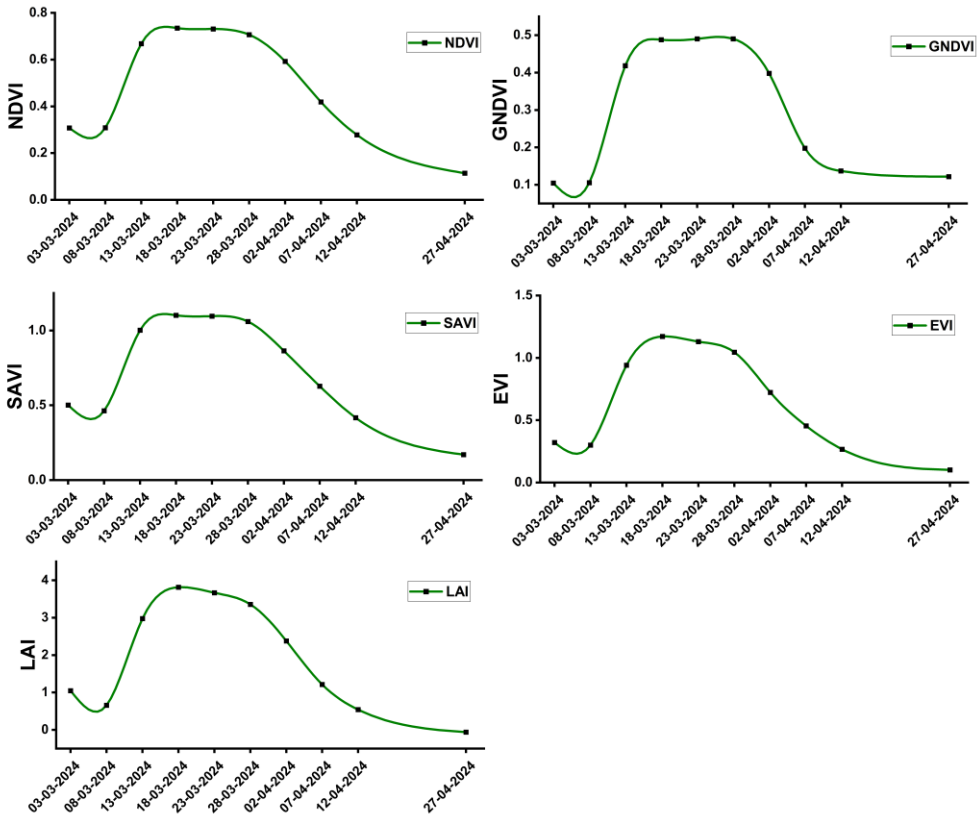

Figure 7. Indices mean value of the paddy crop

Canopy Height: CH of the paddy crop on various temporal dates was extracted from the UAV canopy height model. The median and distribution of canopy height values in different temporal dates are represented in the violin plot (figure 8).

The scatter plot between the measured canopy height (UAV data) and the field measured canopy height reveals a strong linear relationship, as indicated by the linear regression equation which is indicated in figure 9. This equation suggests a close approximation between UAV-derived and field-measured values, with a slope of 0.94 and a small positive intercept (0.03), indicating that the UAV measured canopy height estimates are slightly lower on average than the field measurements but very close to parity. The RMSE of 0.04 further supports the accuracy of the UAV measurements, as it reflects minimal deviation from field values. The high R^2 suggests that 95% of the variation in measured canopy height can be explained by the field measurements, highlighting the effectiveness of UAV based methods in estimating canopy height with high fidelity.

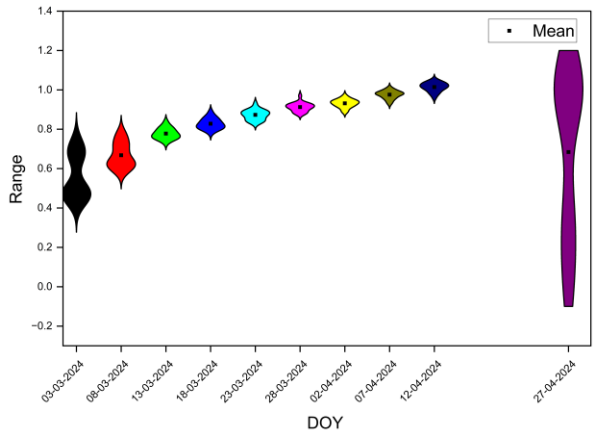

Figure 8. Violin plot representation of canopy height values of paddy crop in various temporal dates

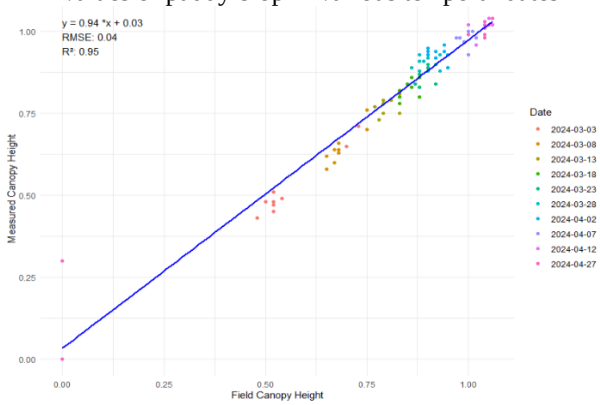

Figure 9. Scatter plot between measured and field canopy height

The scatter plot between the measured canopy height (UAV data) and the field-measured canopy height reveals a strong linear relationship, as indicated by the linear regression equation which is indicated in figure 9. This equation suggests a close approximation between UAV-derived and field-measured values, with a slope of 0.94 and a small positive intercept (0.03), indicating that the UAV measured canopy height estimates are slightly lower on average than the field measurements but very close to parity. The RMSE of 0.04 further supports the accuracy of the UAV measurements, as it reflects minimal deviation from field values. The high R^2 suggests that 95% of the variation in measured canopy height can be explained by the field measurements, highlighting the effectiveness of UAV-based methods in estimating canopy height with high fidelity.

Based on statistical analysis, the linear relationships, RMSE, R^2 values, and Pearson correlation coefficients were computed to determine the accuracy and strength of these relationships and the statistical analysis were represented in the heat maps (figure 9). The relationship between NDVI and SAVI displayed a perfect linear fit, with an equation of y=1.5x and both RMSE and R^2 values at 0 and 1, respectively. The Pearson coefficient of 1 indicates an exact positive correlation, suggesting that SAVI can be predicted directly from NDVI with high reliability. Similarly, the NDVI vs. EVI and NDVI vs. LAI relationships also exhibited strong correlations, with both R^2 and Pearson coefficients exceeding 0.90. For NDVI and EVI, the relationship y=1.52x−0.08 yielded an RMSE of 0.08, while the relationship between NDVI and LAI, y=5.51x−0.71, achieved the same RMSE and strong correlation values. These high correlation metrics indicate a robust association, suggesting that NDVI provides a reliable basis for estimating both EVI and LAI values.

In contrast, NDVI vs. CH, represented by y=0.41x+0.61, showed weaker correlation metrics, with an R^2 of 0.196 and a Pearson coefficient of 0.443. The higher RMSE of 0.25 in this pairing indicates lower predictive accuracy, suggesting that NDVI may not effectively capture changes in canopy height (CH). A similar trend was observed with GNDVI and CH (y=0.56x+0.64), which also yielded an R^2 of 0.202 and a Pearson coefficient of 0.449, demonstrating a modest relationship. These results highlight that while NDVI and GNDVI are excellent predictors for some vegetation indices, they are less effective for canopy height estimation.

Further analysis on the SAVI vs. EVI and SAVI vs. LAI relationships showed high R^2 values of 0.909 and Pearson coefficients of 0.953, indicating robust predictability and similarity between these indices. SAVI vs. CH, however, was found to be less correlated, with a relatively low R^2 of 0.196 and Pearson coefficient of 0.443, further supporting the observation that CH may not correlate as strongly with the vegetation indices considered.

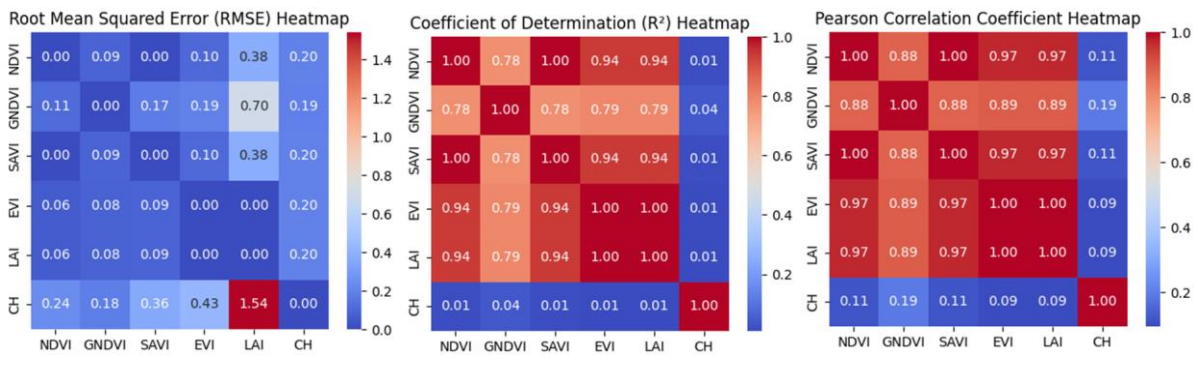

Figure 10. Heat maps a). RMSE, b). R^2, c) Pearson Correlation Coefficient

The EVI vs. LAI relationship achieved perfect accuracy with an R^2 of 1 and Pearson coefficient of 1, signifying that EVI is an excellent predictor of LAI under the conditions studied. However, the EVI vs. CH and LAI vs. CH relationships showed weak correlations, with R^2 values of 0.098 and Pearson coefficients of approximately 0.31, and relatively high RMSE values of 0.43 and 1.54, respectively. This further supports the finding that canopy height has a weaker relationship with other vegetation indices compared to other pairings.

The results demonstrate that NDVI, SAVI, EVI, and GNDVI indices are all effective for monitoring crop biomass and health,

as shown by their strong correlations with each other and with LAI. EVI and SAVI emerge as particularly robust indices, showing very high correlations with LAI, which is critical for monitoring crop canopy characteristics. However, indices like NDVI, GNDVI, SAVI, and EVI exhibited weak correlations with CH (crop height), suggesting that these spectral indices are more suited to measuring crop density, health, and biomass rather than structural parameters like height. This limitation may stem from the fact that crop height is influenced by additional factors not captured by these indices, such as environmental conditions or specific crop growth characteristics. These findings underscore the importance of selecting appropriate indices based on the specific parameter of interest in crop monitoring. For example, EVI and NDVI are suitable for biomass estimation and canopy density but are less effective for predicting structural parameters like height. Integrating other data sources, such as LiDAR or multispectral imaging, could enhance the ability to monitor crop structure in future studies.

5. Conclusion

This study demonstrates the effectiveness of using temporal UAV derived imagery to monitor crop growth and health dynamics through VI's. The UAV orthomosaic images enabled the temporal analysis of indices, which showed significant variations in response to crop development phases. The temporal pattern aligns with physiological changes in crops, with high NDVI and LAI values during peak growth stages indicating optimal photosynthetic activity and dense canopy coverage. Statistical analysis reinforced these observations, with high correlations and low RMSE values for several VIs, confirming that UAV-based methods offer a reliable approximation of crop health metrics.

The results also highlight that NDVI serves as a strong predictor for related indices like SAVI, EVI, and LAI, indicating that these indices can be interchangeably used for monitoring crop biomass and density. Overall, this study validates the utility of UAV-based imagery for crop monitoring, emphasizing the importance of selecting vegetation indices that align with the specific crop parameters of interest. For crop biomass and canopy density assessment, indices like NDVI, EVI, and SAVI are valuable tools, while future research may consider hybrid approaches to capture structural traits like height.

References

Allu, A. R., & Mesapam, S. (2024). Fusion of different multispectral band combinations of Sentinel-2A with UAV imagery for crop classification. Journal of Applied Remote Sensing, 18(01). https://doi.org/10.1117/1.JRS.18.016511

Boegh, E., Soegaard, H., Broge, N., Hasager, C. B., Jensen, N. O., Schelde, K., & Thomsen, A. (2002). Airborne multispectral data for quantifying leaf area index, nitrogen concentration, and photosynthetic efficiency in agriculture. Remote Sensing of Environment, 81(2–3), 179–193. https://doi.org/10.1016/S0034-4257(01)00342-X

de Castro, A. I., Shi, Y., Maja, J. M., & Peña, J. M. (2021). Uavs for vegetation monitoring: Overview and recent scientific contributions. Remote Sensing, 13(11), 1–13.

Garcia-Vasquez, A. C., Mokari, E., Samani, Z., & Fernald, A. (2022). Using UAV-thermal imaging to calculate crop water use and irrigation efficiency in a flood-irrigated pecan orchard. Agricultural Water Management, 272, 107824.

Gerardo, R., & De Lima, I. P. (2023). Applying RGB-Based Vegetation Indices Obtained from UAS Imagery for Monitoring the Rice Crop at the Field Scale: A Case Study in Portugal. Agriculture, 13(10), 1916. https://doi.org/10.3390/agriculture13101916

Huete, A. R. (1988). A soil-adjusted vegetation index (SAVI). Remote Sensing of Environment, 25(3), 295–309. https://doi.org/10.1016/0034-4257(88)90106-X

Jiang, R., Sanchez-Azofeifa, A., Laakso, K., Wang, P., Xu, Y., Zhou, Z., Luo, X., Lan, Y., Zhao, G., & Chen, X. (2021). UAV-based partially sampling system for rapid NDVI mapping in the evaluation of rice nitrogen use efficiency. Journal of Cleaner Production, 289, 125705. https://doi.org/10.1016/j.jclepro.2020.125705

Ma, Y., Chen, H., Zhao, G., Wang, Z., & Wang, D. (2020). Spectral Index Fusion for Salinized Soil Salinity Inversion Using Sentinel-2A and UAV Images in a Coastal Area. IEEE Access, 8, 159595–159608. https://doi.org/10.1109/ACCESS.2020.3020325

Mangewa, L. J., Ndakidemi, P. A., Alward, R. D., Kija, H. K., Bukombe, J. K., Nasolwa, E. R., & Munishi, L. K. (2022). Comparative Assessment of UAV and Sentinel-2 NDVI and GNDVI for Preliminary Diagnosis of Habitat Conditions in Burunge Wildlife Management Area, Tanzania. Earth (Switzerland), 3(3), 769–787.

Ruwanpathirana, P. P., Sakai, K., Jayasinghe, G. Y., Nakandakari, T., Yuge, K., Wijekoon, W. M. C. J., Priyankara, A. C. P., Samaraweera, M. D. S., & Madushanka, P. L. A. (2024). Evaluation of Sugarcane Crop Growth Monitoring Using Vegetation Indices Derived from RGB-Based UAV Images and Machine Learning Models. Agronomy, 14(9), 2059.

Sishodia, R. P., Ray, R. L., & Singh, S. K. (2020). Applications of remote sensing in precision agriculture: A review (Indices vegetativos utilizados na agricultura). Remote Sensing, 12(19), 1–31.

Somvanshi, S. S., & Kumari, M. (2020). Comparative analysis of different vegetation indices with respect to atmospheric particulate pollution using sentinel data. Applied Computing and Geosciences, 7(June), 100032.

Yeom, J., Jung, J., Chang, A., Ashapure, A., Maeda, M., Maeda, A., & Landivar, J. (2019). Comparison of vegetation indices derived from UAV data for differentiation of tillage effects in agriculture. Remote Sensing, 11(13). https://doi.org/10.3390/rs11131548